dairy

MDPI

Article

Effects of Stress of the Endoplasmic Reticulum on Genome-Wide Gene Expression in the Bovine Liver Cell Model BFH12

Eron Bajrami [1], Gaiping Wen [1], Sarah M. Grundmann [1], Robert Ringseis [1,2], Denise K. Gessner [1] and Klaus Eder [1,2,*]

[1] Institute of Animal Nutrition and Nutrition Physiology, Justus Liebig Universität Giessen, Heinrich-Buff-Ring 26-32, 35392 Giessen, Germany; eron.bajrami-2@vetmed.uni-giessen.de (E.B.); gaiping.wen@ernaehrung.uni-giessen.de (G.W.); sarah.grundmann@ernaehrung.uni-giessen.de (S.M.G.); robert.ringseis@ernaehrung.uni-giessen.de (R.R.); denise.gessner@ernaehrung.uni-giessen.de (D.K.G.)

[2] Center of Sustainable Food Systems, Justus Liebig Universität Giessen, Senkenbergstrasse 3, 35390 Giessen, Germany

* Correspondence: klaus.eder@ernaehrung.uni-giessen.de

Abstract

Previous studies have demonstrated that high-yielding dairy cows experience endoplasmic reticulum (ER) stress in the liver during early lactation. To date, most insights into the role of ER stress in metabolism and disease pathophysiology have been derived from rodent and human models. In dairy cattle, however, the specific impact of ER stress on metabolic pathways and its contribution to disease development remain insufficiently characterized. The objective of this study was therefore to investigate the molecular effects of ER stress using a bovine liver cell model (BFH12 cells). ER stress was induced by incubation with Tunicamycin (TM) and Thapsigargin (TG). Molecular responses to ER stress were assessed via a whole-genome array analysis and PCR targeting genes involved in selected metabolic pathways. Incubation with both ER stress inducers resulted in a marked upregulation of genes associated with the unfolded protein response (UPR) within a 4 to 24-h time frame, indicative of the production of robust ER stress in these cells. Unexpectedly, treatment with TM led to a downregulation of numerous genes involved in lipid biosynthesis, including those related to lipogenesis and cholesterol synthesis. Furthermore, incubation with TM and TG induced upregulation of genes involved in fatty acid oxidation and was accompanied by a reduction in intracellular triglyceride concentrations. Genes associated with inflammatory responses were upregulated by both TM and TG, whereas genes encoding antioxidant enzymes were downregulated. Genes involved in ketogenesis did not exhibit a consistent pattern of regulation. Overall, several effects of ER stress previously described in rodent models could not be replicated in this bovine liver cell system. Extrapolating these findings to dairy cows suggests that while ER stress may contribute to hepatic inflammation, it is unlikely to play a significant role in the development of hepatic lipidosis or ketosis.

Keywords: unfolded protein response; liver; cow; lipogenesis; ketogenesis; inflammation

check for updates

Academic Editor: Juan J. Loor

Received: 20 August 2025
Revised: 21 October 2025
Accepted: 24 October 2025
Published: 31 October 2025

Citation: Bajrami, E.; Wen, G.; Grundmann, S.M.; Ringseis, R.; Gessner, D.K.; Eder, K. Effects of Stress of the Endoplasmic Reticulum on Genome-Wide Gene Expression in the Bovine Liver Cell Model BFH12. *Dairy* **2025**, *6*, 64. https://doi.org/10.3390/dairy6060064

Copyright: © 2025 by the authors. Licensee MDPI, Basel, Switzerland. This article is an open access article distributed under the terms and conditions of the Creative Commons Attribution (CC BY) license (https://creativecommons.org/licenses/by/4.0/).

1. Introduction

The periparturient period, defined as the interval spanning three weeks before to three weeks after parturition, constitutes the most critical phase in the reproductive cycle of high-yielding dairy cows. With the onset of lactation, cows experience a pronounced negative energy balance (NEB), driven by a sharp increase in energy demands for milk production coupled with a concurrently reduced feed intake [1]. This NEB triggers extensive lipolysis,

resulting in the mobilization of large quantities of non-esterified fatty acids (NEFA) from adipose tissue. A portion of these NEFA is taken up by the liver. Due to the limited capacity for β-oxidation in hepatic tissue, a substantial fraction of NEFA is re-esterified into triacylglycerols, leading to hepatic triglyceride accumulation and the development of fatty liver [2,3]. Moreover, the elevated rate of gluconeogenesis during early lactation depletes hepatic oxaloacetate, rendering it insufficient to fully condense with acetyl-CoA derived from β-oxidation. Consequently, excess acetyl-CoA is diverted toward ketogenesis, resulting in the formation of ketone bodies and the manifestation of subclinical or clinical ketosis [2,4].

In addition to these metabolic disturbances, the liver is exposed to inflammatory insults, including microbial components (e.g., lipopolysaccharides), pro-inflammatory cytokines, and reactive oxygen species. These insults often originate from infectious diseases such as mastitis and metritis, or from ruminal acidosis, which are prevalent during early lactation [5–8]. Together, these metabolic and inflammatory stressors induce cellular stress responses in hepatic tissue.

Recent studies have demonstrated that, in addition to oxidative stress, endoplasmic reticulum (ER) stress is also activated in the liver shortly after parturition [9,10]. ER stress arises when the protein-folding capacity of the ER is overwhelmed, leading to the accumulation of unfolded or misfolded proteins within the ER lumen [11]. This disruption of ER homeostasis initiates an adaptive signaling cascade known as the unfolded protein response (UPR), which aims to restore ER function through three primary mechanisms: (i) upregulation of ER chaperones to enhance protein folding capacity; (ii) attenuation of global protein translation; and (iii) degradation of aberrant proteins via ER-associated degradation. If these compensatory mechanisms fail, the UPR can trigger apoptotic cell death [12,13].

Beyond these canonical responses, the UPR also modulates lipid biosynthesis, promotes inflammation via activation of nuclear factor kappa B (NF-κB), enhances antioxidant defenses through nuclear factor erythroid 2-related factor 2 (Nrf2), and stimulates the synthesis of fibroblast growth factor 21 (FGF21) [14–16]. FGF21, which is markedly upregulated in dairy cows at parturition and during early lactation, has been proposed as a stress-responsive hormone that regulates key metabolic pathways including fatty acid oxidation, gluconeogenesis, and ketogenesis [17–21]. Based on these observations, ER stress has been implicated in the pathogenesis of metabolic disorders in dairy cows, such as ketosis, hepatic steatosis, and insulin resistance [22].

To date, most insights into the role of ER stress in disease pathophysiology have been derived from rodent and human studies. In humans, ER stress is known to contribute to a wide array of conditions, including diabetes mellitus, cardiovascular disease, stroke, ischemia–reperfusion injury, cancer, neurodegeneration, and hepatic and renal disorders [23,24]. In dairy cows, however, the specific impact of ER stress on metabolic pathways and its contribution to disease development remain poorly understood.

The present study aims to elucidate hepatic pathways in bovine cells that are modulated by ER stress. To this end, we employed the BFH12 cell line, a fetal bovine hepatocyte model previously utilized to investigate bovine hepatic steatosis [24]. ER stress was experimentally induced using tunicamycin (TM) and thapsigargin (TG). TM is a nucleoside antibiotic that inhibits N-linked glycoprotein synthesis, thereby promoting the accumulation of misfolded proteins in the ER. TG, on the other hand, inhibits the sarco/endoplasmic reticulum Ca^{2+}-ATPase, leading to ER stress by depleting intraluminal calcium stores [25,26].

2. Materials and Methods

2.1. Cell Culture

The bovine SV40 large T-antigen-transduced fetal hepatocyte-derived cell line BFH12 was kindly provided by Dr. Axel Schoeniger (Institute of Biochemistry, University of Leipzig, Germany). Cells were cultured in Williams' E medium (Bio&SELL, Nürnberg, Germany). containing 5% heat-inactivated FBS, 2 mM L-alanyl-L-glutamine, 100 nM dexamethasone, 0.2 U/mL insulin (all from Sigma-Aldrich, Taufkirchen, Germany) and 1% penicillin/streptomycin (Th. Geyer, Höxter, Germany) at 37 °C in a humidified atmosphere containing 5% CO_2 [27]. Medium was changed every 2–3 days, and cells were passaged every 7 days using Trypsin-EDTA (3 min at 37 °C). BFH12 cell cultures were regularly tested for *Mycoplasma* spp. contamination using the PCR Venor GeM Classic kit (Miberva Biolabs, Berlin, Germany). For experiments, BFH12 cells were seeded in different cell culture vessels (6-, 24-, 96-well plates), and incubated in culture medium only or culture medium containing either vehicle (0.1% DMSO) or TM or TG (dissolved in DMSO, both from Sigma-Aldrich, Taufkirchen, Germany) at different concentrations and for different time periods as described below and/or indicated in the figure legends. All experiments were performed three times each from different cell-passage numbers (independent experiments). An independent experiment was defined as an experiment performed with cells of a specific passage number and included seeding, treatment, and analysis.

2.2. Cell Viability Assay

BFH12 cells were seeded in 96-well plates at a density of 1×10^4 cells/well, and incubated in culture medium until reaching 70–80% confluency. Subsequently, cells were treated with medium only or medium containing vehicle only or TM or TG at different concentrations (TM: 10, 50, 100, 500, 1000 ng/mL; TG: 10, 50, 100, 250, 500 nM) for 24 h. Subsequently, cell viability was determined by the 3-(4,5-dimethylthiazol-2-yl)-2,5-diphenyltetrazolium bromide (MTT; Sigma-Aldrich, Taufkirchen, Germany) assay as described recently [28]. Viability of BFH12 cells treated with different concentrations of TM or TG is presented as percentage of viability of cells treated with medium only.

2.3. Total RNA Extraction

For RNA extraction, BFH12 cells were seeded in 24-well plates at a density of $2.5–3 \times 10^4$ cells/well and incubated in culture medium until reaching 70–80% confluency. Subsequently, cells were treated with medium only or medium containing vehicle only or TM (100 ng/mL) or TG (100 nM) for different time periods (4, 8, 12, 24 h). The culture medium was aspirated and the cells were washed once with PBS. Total RNA was extracted using TRIzol (Invitrogen, Karlsruhe, Germany) according to manufacturer's instruction and stored at −80 °C. The concentration and purity of total RNA was estimated by measuring the optical density at 260 and 280 nm using a (NanoQuant Plate and Infinite M200 microplate reader, i-control 2.0, Tecan, Männedorf, Switzerland).

2.4. Whole-Genome Transcriptome Analysis

Differential transcriptome analysis was conducted using the Affymetrix Bovine Gene 1.0 ST array (Thermo Fisher Scientific, Waltham, MA, USA) consisting of 526,810 probes, which represent 24,341 genes. Five BFH12 cell total RNA samples per treatment were randomly selected and processed at the Genomics Core Facility "KFB—Center of Excellence for Fluorescent Bioanalytics" (Regensburg, Germany), following the Applied Biosystems GeneChip Whole Transcript (WT) PLUS Reagent Kit User Guide (Thermo Fisher Scientific, Waltham, MA, USA). Prior to processing, RNA quality was assessed using an Agilent 2100 Bioanalyzer (Agilent Technologies, Waldbronn, Germany). The

average OD260/280 ratio and RNA integrity number (RIN) were 1.99 ± 0.01 and 9.7 ± 0.1 (n = 15, mean ± SD), respectively, indicating satisfactory RNA quality. Processing of the raw data (cell intensity files), calculation of summarized probe set signals (in $\log_2$ scale), comparison of fold changes (FC), and determination of significance (p-values) were performed as described previously [29]. Annotation of the gene arrays was performed with the "BovGene-1_0-stv1_Probeset_Release 36" annotation file. The microarray data have been made publicly available in MIAME-compliant format in the NCBI's Gene Expression Omnibus (GEO) repository under GEO Accession number GSE305850 [30]. The raw p-values were adjusted for the number of genes tested using Benjamini and Hochberg's false discovery rate (FDR) to account for multiple comparisons. Differentially expressed transcripts were filtered based on FC > 2.0 or <−2.0 and FDR-adjusted p-value < 0.05 for comparisons between groups TM vs. vehicle only (DMSO) and TG vs. vehicle only (DMSO). Gene Set Enrichment Analysis (GSEA) was conducted using the clusterProfiler R package (v.4.5.1) [31], with genes ranked according to a composite metric combining effect size and statistical significance: $\log_2$(FC) × $-\log_{10}$(FDR-adjusted p-value). GSEA was performed within pathway databases Gene Ontology Biological Process and Reactome using gene sets from the Molecular Signatures Database (MSigDB) [32–34], accessed via the msigdbr package (v.25.1.1) [35], with a focus on *Bos taurus*-specific annotations. Parameters included a minimum gene set size of 10, maximum of 500, and a significance threshold of FDR-adjusted p-value < 0.05. Normalized Enrichment Scores (NES) were computed to account for gene set size and correlations. Enrichment results were visualized as dot plots, displaying the top 20 pathways per database. All analyses were conducted in R (4.5.1) [36].

2.5. Synthesis of cDNA and qPCR Analysis

The cDNA was synthesized from 1.2 µg of total RNA using a master mix containing oligo(dT)18 primer (Eurofins MWG Operon, Ebersberg, Germany), dNTP mix (GeneCraft, Lüdinghausen, Germany), 5× RT reaction buffer and M-MuLV Reverse Transcriptase (both from Thermo Fisher Scientific) in a thermocycler (Biometra, Göttingen, Germany). The qPCR analysis was performed with a Rotor-Gene Q system (Qiagen, Hilden, Germany) as described recently in detail [28]. Gene-specific primer pairs were designed using Primer3 [37], and the Basic Local Alignment Search Tool [38], and synthesized by Eurofins MWG Operon (Ebersberg, Germany). Characteristics of primers are listed in Supplementary Table S1. Calculation of relative mRNA levels with the comparative Ct method using the sample with the lowest Ct value as reference Ct value were carried out as described in a recent publication [28]. Normalization of target gene mRNA levels was carried out using multiple reference genes by the geNorm software (geNorm_v. 3.5, Ghent, Belgium) [39]. Based on M-values and V-values, the normalization factor was calculated as the geometric mean of expression data of *B2M*, *RPL12*, *RPL19*, *RPS9* and *SDHA*. Normalized mRNA levels of cells treated with DMSO alone were set to 1 and means and SD of cells of the other treatments were scaled proportionately.

2.6. Immunoblotting

For immunoblotting, BFH12 cells were seeded in 6-well plates at a density of 2×10^5 cells/well and incubated in culture medium until reaching 70–80% confluency. Subsequently, cells were treated with medium only or medium containing vehicle only or TM (100 ng/mL) or TG (100 nM) for 24 h. Following treatment, medium was aspirated and cells were washed with PBS and harvested using a cell scraper (Sarstedt, Nümbrecht, Germany). The cells were centrifuged for 5 min at 350× g and 4 °C, and the resulting cell pellet was dissolved with 20 µL of RIPA buffer [50 mM Tris, 150 mM NaCl, 10% glycerol, 0.1% SDS, 1% Triton X-100, 1 mM EDTA, 0.5% deoxycholate, 1% protease inhibitor cocktail

(Sigma-Aldrich, Taufkirchen, Germany), 1% phosphatase inhibitor cocktail (PhosSTOP, Sigma-Aldrich, Taufkirchen, Germany); pH 7.5], and incubated on ice for 60 min. The samples were then centrifuged at 12,000× *g* for 15 min and 4 °C and the supernatant/cell lysate was collected for the determination of HSPA5, DDIT3 and Vinculin expression. Protein concentration of cell lysates was determined by the bicinchoninic acid protein assay kit (Interchim, Montluçon, France) with BSA as standard. An amount of 10 µg protein was separated on 10% SDS-PAGE and electro-transferred to a nitrocellulose membrane (Pall Corp, Pensacola, FL, USA). After blocking membranes with 5% non-fat dry milk in TBS-T 0.1% at 4 °C overnight, membranes were incubated with primary antibodies mouse anti-DDIT3 (dilution 1:2000), rabbit anti-HSPA5 (dilution 1:5000) and rabbit anti-Vinculin as reference protein (dilution 1:10,000; all from Thermo Fisher Scientific, Darmstadt, Germany) at 4 °C overnight. The membranes were washed, and then incubated with horseradish peroxidase-conjugated secondary antibodies anti-rabbit-IgG (dilution 1:10,000; Sigma-Aldrich, Taufkirchen, Germany) or anti-mouse-IgG (dilution 1:10,000; Abcam, Cambridge, UK) at RT for 1.5 h. Afterward, blots were developed using ECL Plus (GE Healthcare, München, Germany). The signal intensities of specific bands were detected with a Bio-Imaging system (Syngene, Cambridge, UK) and quantified using Syngene GeneTools software (nonlinear dynamics; Syngene, v.1.8.13.O). Normalized protein levels of cells treated with DMSO alone were set to 1 and means and SD of cells of the other treatments were scaled proportionately.

2.7. Cellular Triglyceride Concentration

BFH12 cells were seeded in 96-well plates at a density of 2–3 × 10^4 cells/well and incubated in culture medium until reaching 70–80% confluency. Subsequently, cells were treated with medium only or medium containing vehicle only or TM (100 ng/mL) or TG (100 nM) for different time periods (4, 8, 12, 24 h). After treatment, the medium was aspirated, the cells were washed twice with PBS, and triglyceride concentration determined using the Triglyceride-Glo assay (Promega, Walldorf, Germany) according to the manufacturer's instruction. Luminescence was measured using an Infinite M 200 microplate reader (Tecan, Mainz, Germany), and triglyceride concentration calculated with a glycerol standard curve. Cellular triglyceride concentration was related to the number of cells. Cell counting was performed automatically using Zeiss Labscope v3.4 software (Carl Zeiss, Jena, Germany). Using the cell number for normalization of triglyceride levels was adequate because it clearly reflected the impairment of cell viability in response to treatment with TM (100 ng/mL) or TG (100 nM). In addition, the cell number was better suitable for normalization than cellular protein levels, because the cell monolayer was partially damaged during the Triglyceride-Glo assay and not the whole cellular protein could be recovered.

2.8. Statistical Analysis

The data were statistically analyzed using Minitab statistical software (release 13.0, Minitab Inc., State College, PA, USA). All data represent the means and SD of three independent experiments. Data (residuals) of each independent experiment were analyzed for normality of distribution (Anderson-Darling test). Because data were statistically analyzed only within each time point but not across different time points, one-way analysis of variance (ANOVA) was applied to evaluate the effect of treatment. For statistically significant F-values, the individual means of the treatment groups were compared using Fisher's multiple range test. Effects were considered statistically significant if $p < 0.05$.

3. Results

3.1. Effect of ER Stress Inducers on BFH12 Cell Viability

Prior to studying the effect of ER stress inducers on BFH12 cell metabolism, the effects of 24 treatment with increasing concentrations of either TM (0–1000 ng/mL) or TG (0–500 nM) on cell viability was investigated. Treatment with increasing concentrations of both ER stress inducers decreased cell viability. While cell viability was not impaired at the lowest TM concentration tested (10 ng/mL) when compared to treatment with vehicle alone, cell viability was impaired by 18%, 20% and >30% at TM concentrations of 50, 100 and ≥500 ng/mL, respectively (Figure 1A). Likewise, the lowest concentration of TG tested (10 nM) did not reduce BFH12 cell viability, whereas TG concentrations of 50, 100, 250 and 500 nM reduced cell viability by approx. 20, 25, 35 and 40%, respectively ($p < 0.05$, Figure 1B). For subsequent experiments investigating the effect of ER stress on BFH12 cell metabolism, TM and TG were used at concentrations of 100 ng/mL and 100 nM, respectively, which was reported to induce ER stress in several other cell types (e.g., FRTL-5 cells [40], MDBK cells [28], IPEC-J2 cells [41]).

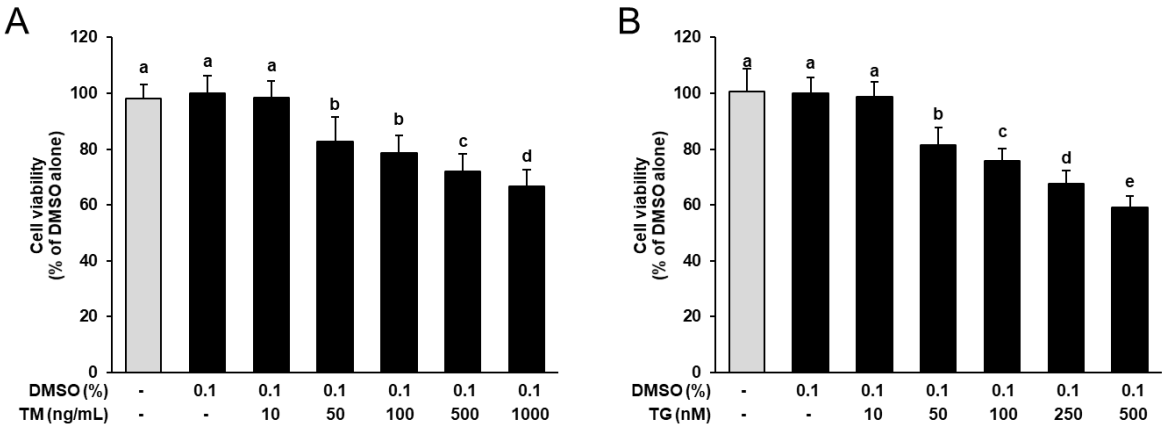

Figure 1. Effect of treatment with increasing concentrations of ER stress inducers TM and TG on BFH12 cell viability. After reaching 70–80% confluency, BFH12 cells were treated with medium only or medium containing vehicle only (0.1% DMSO) or TM (**A**) or TG (**B**) at the concentrations indicated for 24 h. Data are means ± SD from three independent experiments. ^{a,b,c,d,e} Means without a common letter within one time point differ across the treatments, $p < 0.05$.

3.2. Effect of ER Stress Inducers on Indicators of ER Stress in BFH12 Cells

In order to study the induction of ER stress in BFH12 cells, the mRNA of several ER stress target genes involved in the UPR were measured in BFH12 cells treated or not with TM (100 ng/mL) and TG (100 nM) for different time periods (4–24 h). The mRNA levels of all ER stress target genes investigated (*ATF4*, *DDIT3*, *DNAJC3*, *FGF21*, *HSPA5*, *HERPUD1*, *HYOU1*, *PDIA4*) were higher in BFH12 cells treated with TM and TG than in cells treated with vehicle only at all incubation periods ($p < 0.05$, Table 1). Treatment with TM caused the strongest induction of *ATF4*, *DDIT3*, *DNAJC3*, *FGF21*, *HSPA5*, *HERPUD1*, *HYOU1*, *PDIA4* after 12, 12, 24, 4, 12, 8, 24 and 12 h, respectively, compared to treatment with vehicle. TG caused the strongest induction of ATF4, DDIT3, DNAJC3, FGF21, HSPA5, *HERPUD1*, *HYOU1*, *PDIA4* after 4, 12, 12, 4, 12, 12, 12 and 12 h, respectively, compared to treatment with vehicle. Given that most ER stress target genes exhibited peak mRNA expression between 12 and 24 h, BFH12 cells were treated for 24 h in all subsequent experiments.

In line with the markedly elevated *HSPA5* and *DDIT3* mRNA levels, the protein levels of HSPA5 and DDIT3 were markedly higher in BFH12 cells treated for 24 h with TM (8- and 2.4-fold, respectively) and TG (9.5- and 2.5-fold, respectively) than in cells treated with a vehicle (Figure 2A). In addition, treatment of BFH12 cells with TM and TG for 4, 8, 12 and

48 h caused XBP1 splicing, a known effect of ER stress, as evident from the detection of a 129 bp PCR product representing the spliced XBP1 (*sXBP1*) (Figure 2B). The band intensity of *sXBP1* was similar for all treatment periods with TM. In contrast, *sXBP1* band intensity was weaker for treatment with TG for 24 h than treatment with TG for shorter time periods. In agreement with this, the band intensity of the unspliced *XBP1* PCR product (155 bp) was higher after 24 h treatment with TG than after shorter treatment periods with TG. This indicated that *XBP1* splicing was mainly induced by TG between 4 and 12 h of treatment.

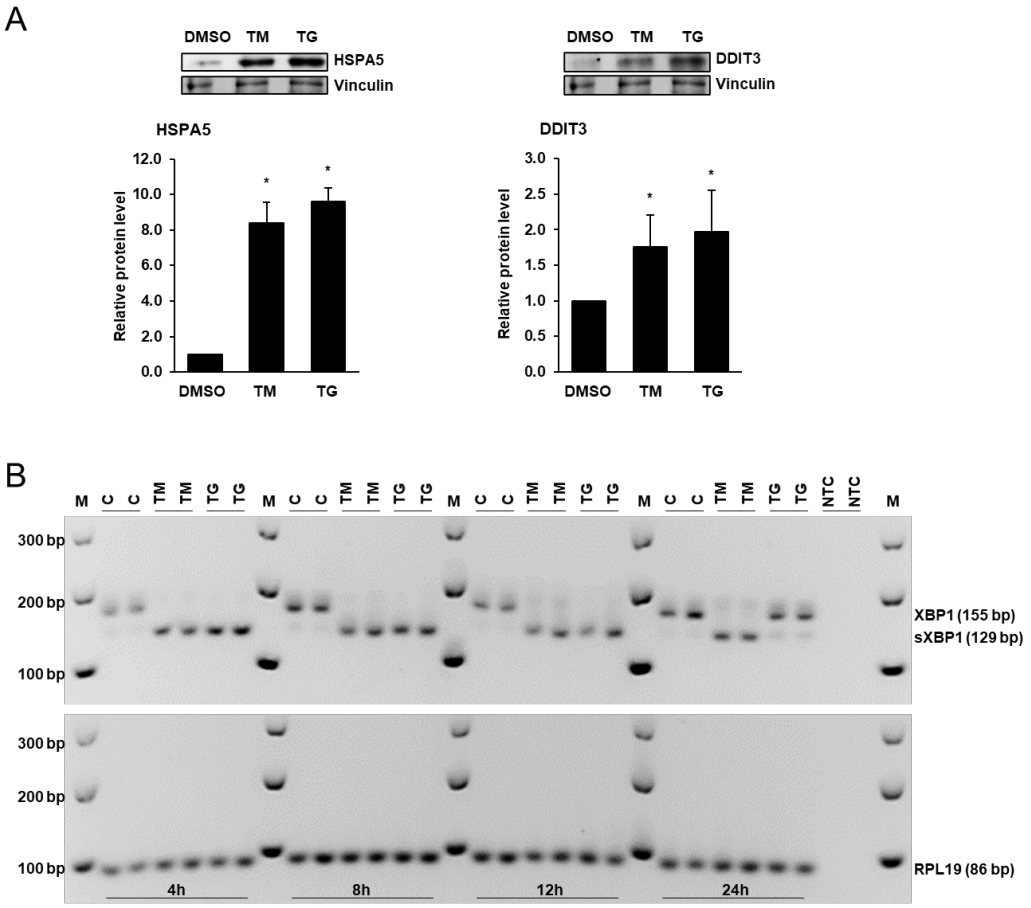

Figure 2. Effect of treatment with ER stress inducers TM and TG on protein levels of ER stress marker genes HSPA5 and DDIT3 (**A**) and *XBP1* splicing (**B**) in BFH12 cells. After reaching 70–80% confluency, BFH12 cells were treated with medium containing either vehicle only (0.1% DMSO) or TM (100 ng/mL) or TG (100 nM) for 24 h (**A**) or 4–24 h (**B**). (**A**) Data are means ± SD from three independent experiments. * Asterisks denote difference from DMSO, $p < 0.05$. Representative immunoblots for HSPA5 and DDIT3 including immunoblots for Vinculin as internal controls are shown above the diagram. (**B**) Representative image from agarose gel electrophoresis of unspliced (155 bp PCR product) and spliced (s) *XBP1* (129 bp PCR product) as detected by conventional PCR. The mRNA expression of *RPL19* served as an internal control.

Table 1. Relative mRNA concentrations of ER stress target genes in BFH12 cells treated with either vehicle (0.1% DMSO), TM (100 ng/mL) or TG (100 nM) for different time periods.

		Time Periods (h)			
Gene	**Treatment**	**4**	**8**	**12**	**24**
ATF4	DMSO	1.00 ± 0.00^{c}	1.00 ± 0.00^{b}	1.00 ± 0.00^{b}	1.00 ± 0.00^{b}
	TM	2.41 ± 0.24^{b}	2.26 ± 0.60^{a}	2.41 ± 0.56^{a}	1.62 ± 0.23^{a}
	TG	3.23 ± 0.45^{a}	2.42 ± 0.52^{a}	2.31 ± 0.52^{a}	1.33 ± 0.14^{a}

Table 1. *Cont.*

		Time Periods (h)			
Gene	**Treatment**	**4**	**8**	**12**	**24**
	DMSO	1.00 ± 0.00 ^{b}	1.00 ± 0.00 ^{c}	1.00 ± 0.00 ^{c}	1.00 ± 0.00 ^{c}
DDIT3	TM	8.17 ± 2.75 ^{a}	10.02 ± 1.60 ^{b}	11.76 ± 2.06 ^{b}	9.65 ± 1.23 ^{a}
	TG	8.19 ± 2.17 ^{a}	15.66 ± 0.71 ^{a}	18.96 ± 1.65 ^{a}	3.29 ± 0.36 ^{b}
	DMSO	1.00 ± 0.00 ^{c}	1.00 ± 0.00 ^{b}	1.00 ± 0.00 ^{c}	1.00 ± 0.00 ^{c}
DNAJC3	TM	2.27 ± 0.37 ^{b}	3.02 ± 0.74 ^{a}	3.95 ± 1.02 ^{b}	4.04 ± 0.46 ^{a}
	TG	3.17 ± 1.04 ^{a}	3.38 ± 0.80 ^{a}	5.20 ± 0.25 ^{a}	3.06 ± 0.01 ^{b}
	DMSO	1.00 ± 0.00 ^{c}	1.00 ± 0.00 ^{c}	1.00 ± 0.00 ^{c}	1.00 ± 0.00 ^{c}
FGF21	TM	11.14 ± 0.90 ^{b}	8.43 ± 0.30 ^{b}	5.17 ± 0.52 ^{b}	4.19 ± 0.99 ^{a}
	TG	14.82 ± 1.18 ^{a}	10.73 ± 1.98 ^{a}	7.95 ± 0.74 ^{a}	1.21 ± 0.47 ^{b}
	DMSO	1.00 ± 0.00 ^{c}	1.00 ± 0.00 ^{c}	1.00 ± 0.00 ^{c}	1.00 ± 0.00 ^{c}
HSPA5	TM	4.71 ± 0.50 ^{b}	12.88 ± 1.28 ^{b}	13.06 ± 2.39 ^{b}	10.55 ± 1.31 ^{a}
	TG	6.63 ± 0.07 ^{a}	13.75 ± 1.47 ^{a}	18.12 ± 3.08 ^{a}	6.69 ± 0.17 ^{b}
	DMSO	1.00 ± 0.00 ^{b}	1.00 ± 0.00 ^{b}	1.00 ± 0.00 ^{c}	1.00 ± 0.00 ^{c}
HERPUD1	TM	9.85 ± 0.72 ^{a}	11.02 ± 1.52 ^{a}	10.94 ± 0.91 ^{b}	6.64 ± 0.61 ^{a}
	TG	9.35 ± 0.62 ^{a}	12.07 ± 1.78 ^{a}	16.82 ± 1.53 ^{a}	3.29 ± 0.37 ^{b}
	DMSO	1.00 ± 0.00 ^{c}	1.00 ± 0.00 ^{c}	1.00 ± 0.00 ^{c}	1.00 ± 0.00 ^{c}
HYOU1	TM	3.57 ± 0.72 ^{b}	6.43 ± 0.82 ^{b}	12.35 ± 0.30 ^{b}	22.10 ± 3.60 ^{a}
	TG	5.52 ± 0.62 ^{a}	14.09 ± 1.35 ^{a}	22.83 ± 1.36 ^{a}	9.01 ± 0.57 ^{b}
	DMSO	1.00 ± 0.00 ^{c}	1.00 ± 0.00 ^{b}	1.00 ± 0.00 ^{c}	1.00 ± 0.00 ^{c}
PDIA4	TM	1.85 ± 0.18 ^{b}	3.78 ± 0.87 ^{a}	5.70 ± 1.42 ^{b}	4.59 ± 0.37 ^{a}
	TG	2.57 ± 0.25 ^{a}	3.83 ± 0.61 ^{a}	7.21 ± 1.76 ^{a}	3.48 ± 1.20 ^{b}

Data are means ± SD from three independent experiments. ^{a,b,c} Means without a common letter within one time point differ across the treatments, $p < 0.05$.

3.3. Effect of ER Stress Inducers on Expression of Genes Involved in Inflammation in BFH12 Cells

In line with the known stimulatory effect of ER stress on inflammation, treatment with TM and TG for 24 h increased mRNA levels of *NFKB1* and *TNF* when compared to treatment with vehicle only ($p < 0.05$, Table 2); *NFKB1* was already upregulated by TM and TG after 4 h of incubation and remained upregulated at later time periods; *TNF* was upregulated only after 8 h of incubation with TM and TG and remained upregulated by both ER stress inducers at later time periods.

Table 2. Relative mRNA concentrations of inflammatory genes in BFH12 cells treated with either vehicle (0.1% DMSO), TM (100 ng/mL) or TG (100 nM) for different time periods.

		Time Periods (h)			
Gene	**Treatment**	**4**	**8**	**12**	**24**
	DMSO	1.00 ± 0.00 ^{b}	1.00 ± 0.00 ^{b}	1.00 ± 0.00 ^{c}	1.00 ± 0.00 ^{c}
NFKB1	TM	1.25 ± 0.43 ^{a}	1.39 ± 0.36 ^{a}	1.97 ± 0.37 ^{a}	1.51 ± 0.27 ^{a}
	TG	1.32 ± 0.25 ^{a}	1.39 ± 0.35 ^{a}	1.23 ± 0.26 ^{b}	1.28 ± 0.25 ^{b}
	DMSO	1.00 ± 0.00 ^{a}	1.00 ± 0.00 ^{b}	1.00 ± 0.00 ^{b}	1.00 ± 0.00 ^{b}
TNF	TM	0.61 ± 0.24 ^{b}	1.41 ± 0.38 ^{a}	1.46 ± 0.38 ^{a}	1.79 ± 0.40 ^{a}
	TG	0.88 ± 0.14 ^{a}	1.43 ± 0.48 ^{a}	1.35 ± 0.49 ^{a}	1.96 ± 0.20 ^{a}

Data are means ± SD from three independent experiments. ^{a,b,c} Means without a common letter within one time point differ across the treatments, $p < 0.05$.

3.4. Effect of ER Stress Inducers on the Transcriptome of BFH12 Cells

In order to evaluate the effect of ER stress inducers on BFH12 cell metabolism, genome-wide transcriptome analysis was carried out following treatment of cells with TM (100 ng/mL) or TG (100 nM) for 24 h. When comparing BFH12 cells treated with

TM and those treated with vehicle (0.1% DMS) (TM vs. control), a total of 216 transcripts were differentially regulated according to the two-filter criteria (FC > 2 or <−2, FDR-adjusted $p < 0.05$); of those, 139 transcripts were upregulated and 77 transcripts were downregulated in cells treated with TM compared to those treated with vehicle (Figure 3A). Amongst the upregulated transcripts, the 10 most strongly regulated transcripts in response to TM were in decreasing order of their FC (in brackets): *CYP3A4* (10.54), *RCAN1* (10.08), *CCDC39* (9.85), *TNFSF18* (8.74), *SYT4* (7.83), *IFIT1* (7.25), *DNAJB9* (5.18), *PTGS2* (5.12), *DDIT3* (5.04) and *DERL3* (4.99). The 10 most strongly downregulated transcripts in response to TM were in increasing order of their FC (in brackets): *C15H11orf34* (−10.47), *HMGCS1* (−6.9), *LRRN4* (−6.2), *CXCL9* (−5.82), *FABP3* (−4.79), *CA3* (−4.73), *CXCL11* (−4.3), *KRT6A* (−4.05), *SQLE* (−3.96) and *FDFT1* (−3.84). The FC and FDR-adjusted *p*-value of all differentially expressed transcripts between TM vs. control are listed in Supplementary Table S2.

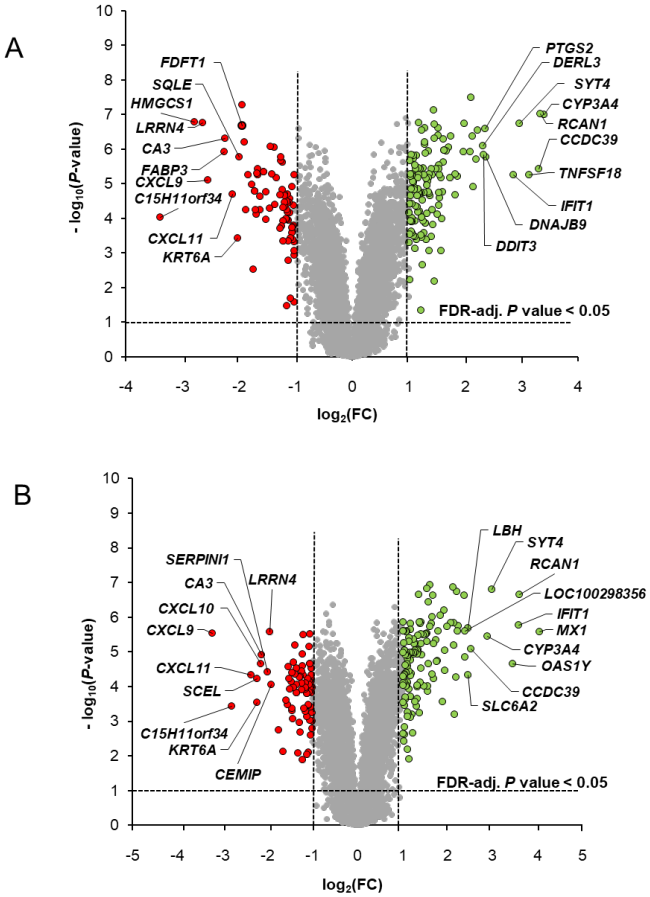

Figure 3. Volcano plots showing the differentially regulated transcripts between BFH12 cells treated with TM vs. DMSO (**A**) and BFH12 cells treated with TG vs. DMSO (**B**). The double filtering criteria are indicated by horizontal (FDR-adjusted *p*-value < 0.05) and vertical (FC: >$\log_2(2.0)$ or <$\log_2(-2.0)$) dashed lines. Transcripts in the upper left and the upper right corner represent the downregulated and the upregulated transcripts, respectively.

Considering the same filter criteria as above, a similar number of differentially expressed transcripts, namely 215, was identified for the comparison TG vs. control. Out of these, 140 were upregulated and 75 were downregulated in cells treated with TG compared to those treated with vehicle (Figure 3B). The 10 most strongly upregulated transcripts in response to TG were in decreasing order of their FC (in brackets): *MX1* (16.55), *RCAN1* (12.13), *IFIT1* (11.95), *OAS1Y* (11.0), *SYT4* (7.97), *CYP3A4* (7.38), *CCDC39* (5.75), *LBH* (5.51), *SLC6A2* (5.22) and *LOC100298356* (5.22). In contrast, the 10 most strongly

downregulated transcripts in response to TG were in increasing order of their FC (in brackets): *CXCL9* (−9.35), *C15H11orf34* (−6.95), *CXCL11* (−5.12), *KRT6A* (−4.96), *SCEL* (−4.67), *CXCL10* (−4.44), *CA3* (−4.39), *SERPINI1* (−4.0), *LRRN4* (−3.84) and *CEMIP* (−3.77). The FC and FDR-adjusted *p*-value of all differentially expressed transcripts between TG vs. control are listed in Supplementary Table S3.

Comparing the top 10 transcripts regulated by TM and TG, five (*CYP3A4*, *RCAN1*, *CCDC39*, *SYT4*, *IFIT1*) and six genes (*KRT6A*, *CXCL11*, *CA3*, *CXCL9*, *LRRN4*, *C15H11orf34*) were found to be upregulated and downregulated, respectively, by both TM and TG. In line with the activation of ER stress by TM and TG, a large number of ER stress-regulated genes were identified amongst the differentially expressed genes (Table 3); a total of 15 and 16 known ER stress target genes were found to be regulated >2-fold in BFH12 cells treated with TM and TG, respectively.

Table 3. Regulation of ER stress target genes according to microarray analysis in BFH12 cells treated with either vehicle (0.1% DMSO), TM (100 ng/mL) or TG (100 nM) for 24 h.

ER Stress Target Gene	TM vs. DMSO FC	TG vs. DMSO FC
DNAJB9	5.18	4.43
DDIT3	5.04	4.41
DERL3	4.99	4.75
TRIB3	4.43	3.24
HERPUD1	4.32	4.35
HYOU1	3.93	4.23
NUPR1	3.66	3.35
CHAC1	2.93	2.14
DNAJB11	2.87	3.16
DNAJC3	2.76	2.22
MANF	2.75	2.57
PDIA4	2.73	3.05
PPP1R15A	2.28	2.56
DERL2	2.21	2.05
FICD	2.12	-
ATF6	-	2.08
EDEM1	-	2.14

3.5. Pathways Affected by ER Stress Inducers Based on Their Effects on the Transcriptome of BFH12 Cells

In order to identify pathways affected by ER stress inducers, GSEA was performed within GO biological process and Reactome pathways databases. In BFH12 cells treated with TM, the most enriched upregulated biological processes were response to endoplasmic reticulum stress, ERAD pathway and regulation of endoplasmic reticulum stress, whereas the most enriched downregulated biological processes were the sterol biosynthetic process, ribonucleoprotein complex biogenesis and steroid biosynthetic process (Figure 4A). The most enriched upregulated Reactome pathways were unfolded protein response UPR and IRE1 activates chaperones and the most enriched downregulated Reactome pathways were metabolism of steroids, regulation of cholesterol biosynthesis by SREBP SREBF and mRNA splicing (Figure 4B).

Likewise, in BFH12 cells treated with TG, the most enriched upregulated biological processes were response to endoplasmic reticulum stress, regulation of endoplasmic reticulum stress and ERAD pathway (Figure 5A), and the most enriched upregulated Reactome pathways were unfolded protein response UPR and IRE1 activates chaperones (Figure 5B). The most enriched downregulated biological processes were the ribonucleoprotein complex

biogenesis, ribosome biogenesis and rRNA metabolic process, and the most enriched downregulated Reactome pathways were processing of capped intron containing pre-mRNA, rRNA processing and mRNA splicing.

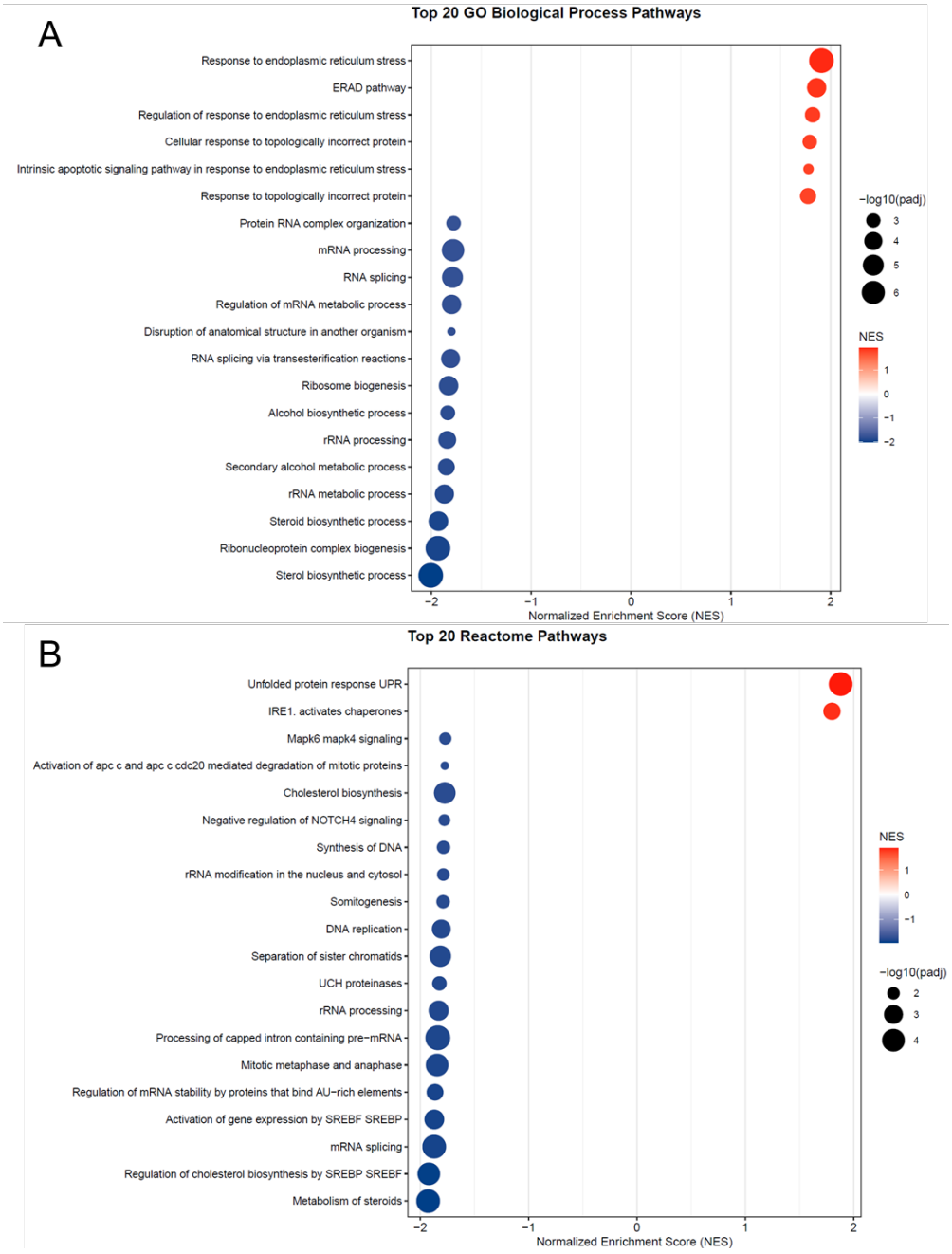

Figure 4. Top 20 significantly enriched Gene Ontology biological processes (**A**) and Reactome pathways (**B**) identified by GSEA. The Normalized Enrichment Score (NES) reflects both the magnitude and direction of pathway enrichment. Positive NES values (red) indicate pathways upregulated in cells treated with ER stress inducer tunicamycin (TM), while negative NES values (blue) indicate downregulated pathways. Point size represents the statistical significance of enrichment ($-\log_{10}$ FDR-adjusted p-value). All pathways shown have adjusted p-value < 0.05.

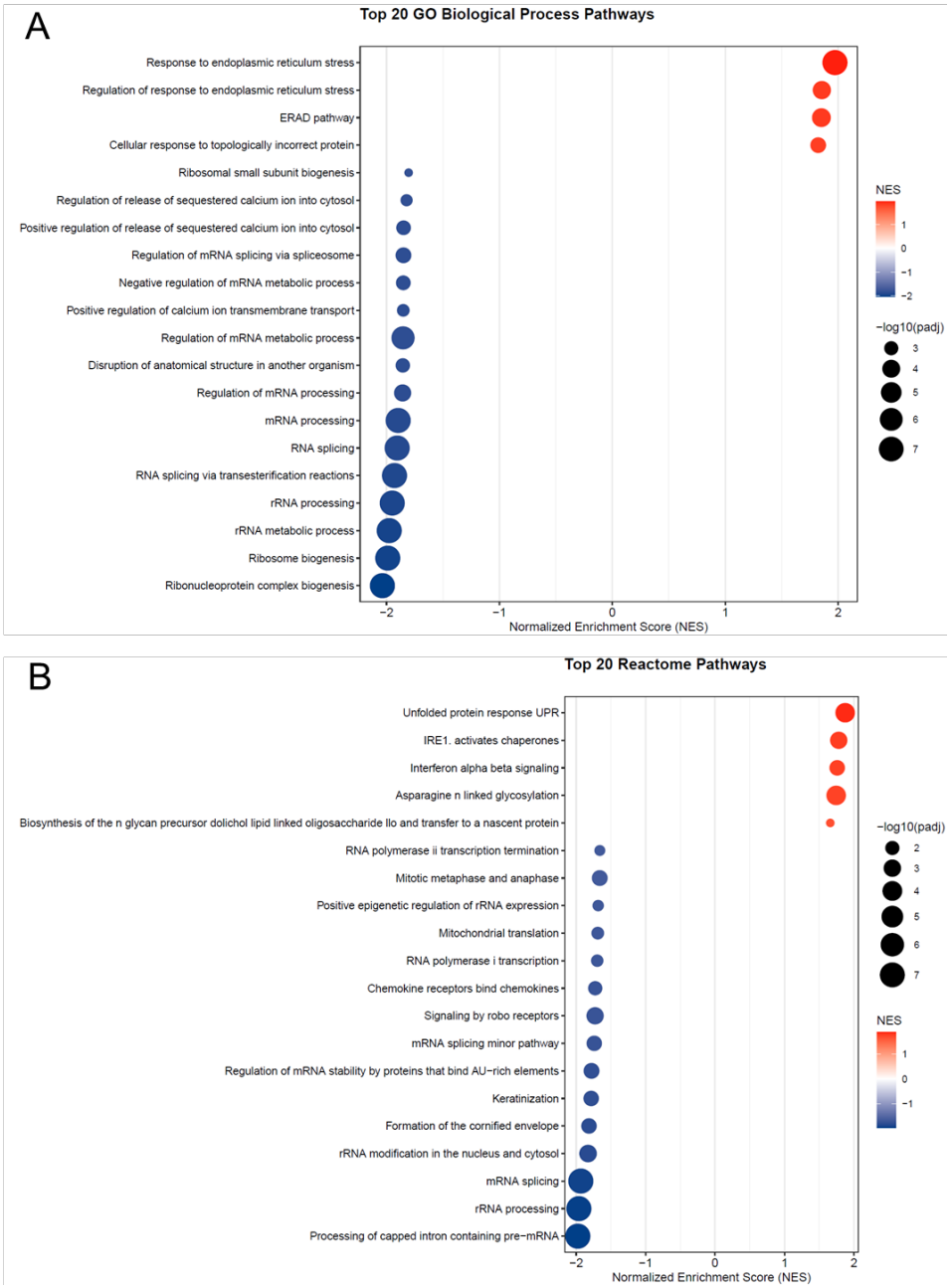

Figure 5. Top 20 significantly enriched Gene Ontology biological processes (**A**) and Reactome pathways (**B**) identified by GSEA. The Normalized Enrichment Score (NES) reflects both the magnitude and direction of pathway enrichment. Positive NES values (red) indicate pathways upregulated in cells treated with ER stress inducer thapsigargin (TG), while negative NES values (blue) indicate downregulated pathways. Point size represents the statistical significance of enrichment ($-\log_{10}$ FDR-adjusted *p*-value). All pathways shown have adjusted *p*-value < 0.05.

3.6. Effect of ER Stress Inducers on Expression of Genes Involved in Lipid Synthesis in BFH12 Cells

Considering that GSEA revealed that the genes downregulated by TM were mainly involved in sterol biosynthetic process, genes of these pathways were filtered from the list of genes downregulated by TM. Those genes were in increasing order of their FC: *HMGCS1* (−6.9), *SQLE* (−3.96), *FDFT1* (−3.84), *SCD* (−3.71), *FADS2* (−3.24), *LDLR* (−3.15), *FDPS* (−2.94), *IDI1* (−2.85), *HMGCR* (−2.7), *LSS* (−2.66), *DHCR24* (−2.58), *ACAT2* (−2.39) and *FASN* (−2.37). None of these genes were found to be downregulated by TG. To confirm this finding from genome-wide transcriptome analysis, the mRNA levels of a set of genes

involved in fatty acid/triglyceride and cholesterol synthesis were determined in BFH12 cells treated or not with TM (100 ng/mL) and TG (100 nM) for different time periods (4–24 h). The mRNA levels of genes involved in fatty acid synthesis investigated (*ACLY*, *ELOVL6*, *FASN*, *ME1*, *ME2*, *SCD*) were markedly reduced in BFH12 cells treated with TM for 24 h when compared to cells treated with vehicle only ($p < 0.05$, Table 4); time-course analysis revealed that these genes were already downregulated by TM at 4 h (*ME1*, *ME2*) and 8 h (*ACLY*, *FASN*, *SCD*, *ELOVL6*) and remained downregulated at 12 h and 24 h. In contrast to TM, the mRNA levels of these genes were either not (*ACLY*, *ME1*, *ME2*, *SCD*) oder only slightly reduced (*FASN*, *ELOVL6*) in BFH12 cells treated with TG for 24 h when compared to cells treated with vehicle only ($p < 0.05$, Table 4); at earlier time points, no consistent regulation of these genes by TG was seen; while *ACLY* and *SCD* were even upregulated at 4 h, *ME1* and *ME2* were downregulated at 4 h and *FASN* and *ELOVL6* were not regulated at 4 h when compared to cells treated with vehicle. The mRNA levels of genes involved in cholesterol homeostasis (*HMGCR*, *LDLR*, *MVK*) were downregulated by TM as early as 4 h (*MVK*) and 8 h (*HMGCR*, *LDLR*) and remained downregulated even stronger at later time-points (12 and 24 h) when compared to control cells ($p < 0.05$, Table 4). In BFH12 cells treated with TG, the mRNA levels of *HMGCR* and *LDLR* were markedly upregulated and that of *MVK* was not regulated at earlier treatment points (4 and 8 h), whereas these genes were not regulated at 12 h and only slightly regulated (*HMGCR*, *MVK*: down, *LDLR*: up) at 24 h.

Table 4. Relative mRNA concentrations of genes involved in fatty acid synthesis and cholesterol homeostasis in BFH12 cells treated with either vehicle (0.1% DMSO), TM (100 ng/mL) or TG (100 nM) for different time periods.

		Time Periods (h)			
Gene	**Treatment**	**4**	**8**	**12**	**24**
Fatty acid synthesis					
	DMSO	1.00 ± 0.00^{b}	1.00 ± 0.00^{a}	1.00 ± 0.00^{a}	1.00 ± 0.00^{a}
ACLY	TM	0.88 ± 0.08^{b}	0.51 ± 0.08^{c}	0.49 ± 0.08^{b}	0.38 ± 0.10^{b}
	TG	1.49 ± 0.27^{a}	0.81 ± 0.20^{b}	0.51 ± 0.07^{b}	0.96 ± 0.05^{a}
	DMSO	1.00 ± 0.00	1.00 ± 0.00^{a}	1.00 ± 0.00^{a}	1.00 ± 0.00^{a}
ELOVL6	TM	0.98 ± 0.22	0.61 ± 0.09^{b}	0.63 ± 0.08^{b}	0.25 ± 0.07^{c}
	TG	0.91 ± 0.08	0.72 ± 0.00^{b}	0.92 ± 0.04^{a}	0.70 ± 0.23^{b}
	DMSO	1.00 ± 0.00	1.00 ± 0.00^{a}	1.00 ± 0.00^{a}	1.00 ± 0.00^{a}
FASN	TM	1.04 ± 0.21	0.51 ± 0.13^{b}	0.74 ± 0.15^{b}	0.34 ± 0.06^{c}
	TG	1.06 ± 0.21	0.72 ± 0.17^{b}	0.74 ± 0.11^{b}	0.69 ± 0.19^{b}
	DMSO	1.00 ± 0.00^{a}	1.00 ± 0.00^{a}	1.00 ± 0.00^{ab}	1.00 ± 0.00^{ab}
ME1	TM	0.70 ± 0.14^{b}	0.82 ± 0.23^{b}	0.84 ± 0.14^{b}	0.83 ± 0.07^{b}
	TG	0.75 ± 0.03^{b}	1.16 ± 0.05^{a}	1.20 ± 0.26^{a}	1.35 ± 0.02^{a}
	DMSO	1.00 ± 0.00^{a}	1.00 ± 0.00^{a}	1.00 ± 0.00^{a}	1.00 ± 0.00^{a}
ME2	TM	0.77 ± 0.06^{b}	0.79 ± 0.06^{b}	0.70 ± 0.12^{b}	0.75 ± 0.02^{b}
	TG	0.79 ± 0.19^{b}	0.77 ± 0.06^{b}	0.77 ± 0.09^{b}	0.87 ± 0.13^{a}
	DMSO	1.00 ± 0.00^{c}	1.00 ± 0.00^{b}	1.00 ± 0.00^{b}	1.00 ± 0.00^{a}
SCD	TM	1.33 ± 0.05^{b}	0.62 ± 0.02^{c}	0.46 ± 0.10^{c}	0.31 ± 0.07^{b}
	TG	3.07 ± 0.38^{a}	2.84 ± 0.65^{a}	2.20 ± 0.14^{a}	0.97 ± 0.07^{a}
Cholesterol synthesis and uptake					
	DMSO	1.00 ± 0.00^{b}	1.00 ± 0.00^{b}	1.00 ± 0.02^{a}	1.00 ± 0.00^{a}
HMGCR	TM	0.80 ± 0.12^{b}	0.60 ± 0.08^{c}	0.53 ± 0.02^{b}	0.30 ± 0.07^{b}
	TG	2.32 ± 0.48^{a}	1.98 ± 0.72^{a}	1.01 ± 0.03^{a}	0.75 ± 0.09^{b}
	DMSO	1.00 ± 0.00^{b}	1.00 ± 0.00^{b}	1.00 ± 0.00^{a}	1.00 ± 0.00^{b}
LDLR	TM	0.94 ± 0.16^{b}	0.65 ± 0.06^{c}	0.43 ± 0.16^{b}	0.26 ± 0.09^{c}
	TG	2.37 ± 0.39^{a}	2.12 ± 0.44^{a}	0.99 ± 0.26^{a}	1.28 ± 0.24^{a}

Table 4. *Cont.*

		Time Periods (h)			
Gene	**Treatment**	**4**	**8**	**12**	**24**
MVK	DMSO	1.00 ± 0.00 [a]	1.00 ± 0.00 [a]	1.00 ± 0.00 [a]	1.00 ± 0.00 [a]
	TM	0.78 ± 0.07 [b]	0.73 ± 0.13 [b]	0.69 ± 0.11 [b]	0.65 ± 0.19 [b]
	TG	0.96 ± 0.19 [a]	0.93 ± 0.13 [a]	0.99 ± 0.13 [a]	0.67 ± 0.05 [b]

Data are means ± SD from three independent experiments. [a,b,c] Means without a common letter within one time point differ across the treatments, $p < 0.05$.

3.7. Effect of ER Stress Inducers on Expression of Genes Involved in Fatty Acid Oxidation in BFH12 Cells

Treatment of BFH12 cells with TM for 24 h had no effect on the mRNA levels of *ACADL* and *ACADVL* but increased those of *CPT1A* and *CPT1B* compared to treatment with vehicle ($p < 0.05$, Table 5); after shorter incubation periods with TM, the mRNA levels of *ACADL* and *ACADVL* were either reduced (*ACADL*: 4 and 12 h) or increased (*ACADVL*: 8 and 12 h). The mRNA levels of *CPT1A* and *CPT1B* were upregulated by TM also at earlier incubation periods (*CPT1A*: 8 and 12 h; *CPT1B*: 4 and 12 h). Treatment with TG for 24 h increased mRNA levels of *ACADL*, *ACADVL*, *CPT1A* and *CPT1B* ($p < 0.05$, Table 5); while *ACADVL* and *CPT1A* were upregulated already at 4 h and remained upregulated up to 24 h of treatment, *ACADL* was not upregulated at earlier time periods and *CPT1B* only at 12 h and longer time periods.

Table 5. Relative mRNA concentrations of genes involved in fatty acid oxidation in BFH12 cells treated with either vehicle (0.1% DMSO), TM (100 ng/mL) or TG (100 nM) for different time periods.

		Time Periods (h)			
Gene	**Treatment**	**4**	**8**	**12**	**24**
ACADL	DMSO	1.00 ± 0.00 [a]	1.00 ± 0.00	1.00 ± 0.00 [a]	1.00 ± 0.00 [b]
	TM	0.68 ± 0.16 [b]	0.98 ± 0.02	0.69 ± 0.18 [b]	0.92 ± 0.06 [b]
	TG	0.81 ± 0.20 [b]	0.99 ± 0.12	0.88 ± 0.11 [a]	1.24 ± 0.17 [a]
ACADVL	DMSO	1.00 ± 0.00 [b]	1.00 ± 0.00 [b]	1.00 ± 0.00 [b]	1.00 ± 0.00 [b]
	TM	0.88 ± 0.11 [b]	1.21 ± 0.44 [a]	1.36 ± 0.07 [a]	0.86 ± 0.02 [b]
	TG	1.24 ± 0.02 [a]	1.38 ± 0.20 [a]	1.35 ± 0.17 [a]	1.63 ± 0.69 [a]
CPT1A	DMSO	1.00 ± 0.00 [b]	1.00 ± 0.00 [b]	1.00 ± 0.00 [c]	1.00 ± 0.00 [b]
	TM	1.14 ± 0.03 [b]	1.72 ± 0.16 [a]	1.30 ± 0.10 [b]	1.39 ± 0.20 [a]
	TG	1.85 ± 0.27 [a]	1.54 ± 0.13 [a]	1.59 ± 0.46 [a]	1.80 ± 0.67 [a]
CPT1B	DMSO	1.00 ± 0.00 [b]	1.00 ± 0.00	1.00 ± 0.00 [b]	1.00 ± 0.00 [b]
	TM	1.23 ± 0.18 [a]	1.03 ± 0.31	1.31 ± 0.15 [a]	1.41 ± 0.04 [a]
	TG	0.89 ± 0.13 [b]	0.92 ± 0.20	1.22 ± 0.09 [a]	1.36 ± 0.04 [a]

Data are means ± SD from three independent experiments. [a,b,c] Means without a common letter within one time point differ across the treatments, $p < 0.05$.

3.8. Effect of ER Stress Inducers on Expression of Genes Involved in Ketone Body Synthesis in BFH12 Cells

Treatment of BFH12 cells with TM and TG for 4–24 h decreased the mRNA level of *ACAT1* compared to treatment with DMSO ($p < 0.05$, Table 6). In contrast, the mRNA level of *HMGCL* was increased following treatment with TM and TG for 8–24 h compared to treatment with DMSO ($p < 0.05$, Table 6).

Table 6. Relative mRNA concentrations of genes involved in ketone body synthesis in BFH12 cells treated with either vehicle (0.1% DMSO), TM (100 ng/mL) or TG (100 nM) for different time periods.

		Time Periods (h)			
Gene	**Treatment**	**4**	**8**	**12**	**24**
ACAT1	DMSO	1.00 ± 0.00 ^{a}	1.00 ± 0.00 ^{a}	1.00 ± 0.00 ^{a}	1.00 ± 0.00 ^{a}
	TM	0.80 ± 0.12 ^{b}	0.81 ± 0.02 ^{b}	0.89 ± 0.14 ^{b}	0.78 ± 0.05 ^{b}
	TG	0.64 ± 0.08 ^{b}	0.81 ± 0.13 ^{b}	0.72 ± 0.05 ^{b}	0.74 ± 0.13 ^{b}
HMGCL	DMSO	1.00 ± 0.00 ^{b}	1.00 ± 0.00 ^{b}	1.00 ± 0.00 ^{b}	1.00 ± 0.00 ^{b}
	TM	0.95 ± 0.18 ^{b}	1.63 ± 0.31 ^{a}	1.58 ± 0.50 ^{a}	1.61 ± 0.05 ^{a}
	TG	1.21 ± 0.03 ^{a}	1.92 ± 0.23 ^{a}	1.30 ± 0.02 ^{a}	1.44 ± 0.38 ^{a}

Data are means ± SD from three independent experiments. ^{a,b} Means without a common letter within one time point differ across the treatments, $p < 0.05$.

3.9. Effect of ER Stress Inducers on Expression of Antioxidant Genes in BFH12 Cells

Treatment of BFH12 cells with TM and TG for 24 h reduced the mRNA levels of antioxidant genes (*CAT*, *GPX3*, *NQO1*, *SOD1*) when compared to treatment with vehicle ($p < 0.05$, Table 7); TM decreased the mRNA levels of all these genes already after 4 h (*NQO1*) or 8 h (*CAT*, *GPX3*, *SOD1*); treatment with TG decreased the mRNA levels of *CAT*, *GPX3*, *NQO1* and *SOD1* as early as 4 h, 12 h, 4 h and 8 h, respectively.

Table 7. Relative mRNA concentrations of genes involved in antioxidant defense in BFH12 cells treated with either vehicle (0.1% DMSO), TM (100 ng/mL) or TG (100 nM) for different time periods.

		Time Periods (h)			
Gene	**Treatment**	**4**	**8**	**12**	**24**
CAT	DMSO	1.00 ± 0.00 ^{a}	1.00 ± 0.00 ^{a}	1.00 ± 0.00 ^{a}	1.00 ± 0.00 ^{a}
	TM	1.02 ± 0.20 ^{a}	0.83 ± 0.06 ^{b}	0.77 ± 0.14 ^{b}	0.77 ± 0.17 ^{b}
	TG	0.79 ± 0.11 ^{b}	0.58 ± 0.13 ^{b}	1.18 ± 0.06 ^{a}	0.82 ± 0.12 ^{b}
GPX3	DMSO	1.00 ± 0.00 ^{b}	1.00 ± 0.00 ^{a}	1.00 ± 0.00 ^{a}	1.00 ± 0.00 ^{a}
	TM	0.96 ± 0.09 ^{b}	0.78 ± 0.05 ^{b}	0.83 ± 0.18 ^{b}	0.81 ± 0.25 ^{b}
	TG	1.32 ± 0.33 ^{a}	0.93 ± 0.12 ^{a}	0.74 ± 0.20 ^{b}	0.75 ± 0.20 ^{b}
NQO1	DMSO	1.00 ± 0.00 ^{a}	1.00 ± 0.00 ^{a}	1.00 ± 0.00 ^{a}	1.00 ± 0.00 ^{a}
	TM	0.57 ± 0.00 ^{c}	0.62 ± 0.06 ^{b}	0.83 ± 0.15 ^{b}	0.45 ± 0.16 ^{c}
	TG	0.84 ± 0.03 ^{b}	0.96 ± 0.12 ^{a}	0.72 ± 0.29 ^{b}	0.62 ± 0.20 ^{b}
SOD1	DMSO	1.00 ± 0.00	1.00 ± 0.00 ^{a}	1.00 ± 0.00 ^{a}	1.00 ± 0.00 ^{a}
	TM	1.05 ± 0.12	0.81 ± 0.28 ^{b}	0.82 ± 0.11 ^{b}	0.63 ± 0.14 ^{b}
	TG	0.93 ± 0.05	0.79 ± 0.30 ^{b}	0.63 ± 0.18 ^{c}	0.83 ± 0.14 ^{b}

Data are means ± SD from three independent experiments. ^{a,b,c} Means without a common letter within one time point differ across the treatments, $p < 0.05$.

3.10. Effect of ER Stress Inducers on Cellular Triglyceride Concentration in BFH12 Cells

In order to explore if the effects of ER stress inducers on the expression of genes involved in lipid metabolism affected cellular lipid levels, the concentration of triglycerides was determined in BFH12 cells treated or not with TM (100 ng/mL) and TG (100 nM) for different time periods (4–24 h). Treatment with TM and TG for 12 and 24 h decreased cellular triglyceride concentration compared to treatment with vehicle alone ($p < 0.05$, Figure 6). After 4 h of treatment, the cellular triglyceride concentration was decreased in BFH12 cells treated with TG but not with TM. Treatment with TM and TG for 8 h had no effect on cellular triglyceride concentration compared to treatment with vehicle.

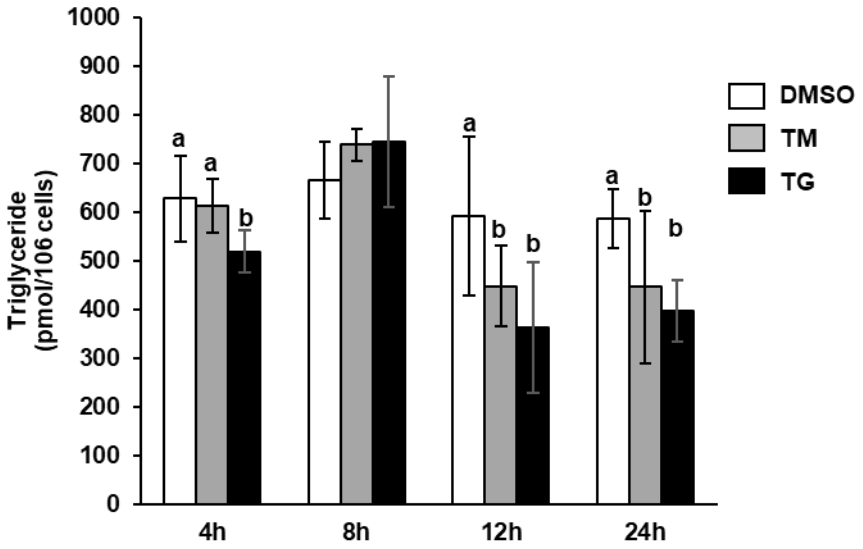

Figure 6. Effect of treatment with ER stress inducers TM and TG on cellular concentration of triglycerides in BFH12 cells. After reaching 70–80% confluency, BFH12 cells were treated with medium containing either vehicle only (0.1% DMSO) or TM (100 ng/mL) or TG (100 nM) for 4–24 h. Data are means ± SD from three independent experiments. ^{a,b} Means without a common letter within one time point differ across the treatments, $p < 0.05$.

4. Discussion

Previous studies have demonstrated that ER stress is induced in the liver of dairy cows during the transition period, leading to activation of the UPR [9,10]. However, the precise molecular effects of ER stress in bovine hepatocytes remain largely unexplored. Based on findings from rodent models and obese humans, it was hypothesized that ER stress may contribute to the pathogenesis of common metabolic disorders in dairy cows, such as hepatic steatosis and ketosis [22]. To investigate the effects of ER stress at the cellular level, we employed the bovine hepatic cell line BFH12, which has previously been used to study the impact of saturated fatty acids on the activation of peroxisome proliferator-activated receptors and lipid accumulation [24,42]. It has been shown that BFH12 cells accumulate lipids upon incubation with saturated fatty acids, making them a suitable in vitro model for studying bovine hepatic steatosis [24].

To examine the molecular consequences of ER stress in bovine hepatocytes, cells were treated with the well-established ER stress inducers TM and TG. As expected and consistent with previous studies, both compounds induced a dose-dependent reduction in cell viability, likely due to apoptosis triggered by prolonged UPR activation. In line with earlier investigations, we selected TM and TG concentrations that maintained cell viability just below 80% [28,40].

To identify metabolic pathways affected by UPR activation, we performed transcriptome analysis on cells incubated with TM or TG for 24 h. Additionally, we quantified mRNA levels of selected metabolic genes over a time course of 4 to 24 h to assess temporal dynamics. Expression analysis of canonical UPR target genes and alternative splicing of XBP1 confirmed robust activation of the UPR by both stressors. The time-course data revealed that UPR activation was pronounced as early as 4 h post-treatment and persisted for at least 24 h. Transcriptomic profiling further validated strong UPR induction, with UPR-associated pathways, such as ERAD pathway and IRE1 activates chaperones, being among the most enriched upregulated biological processes and Reactome pathways following treatment with either TM or TG. In addition, several pathways dealing with RNA processing, such as rRNA processing and mRNA splicing were amongst the most enriched downregulated pathways, in BFH12 cells treated with TM and TG—effects which

reflect a major consequence of ER stress induction, namely the attenuation of global protein translation [12,13].

A striking observation from whole-genome transcriptome analysis was the downregulation of numerous genes involved in cholesterol and fatty acid biosynthesis, such as *HMGCS1*, *SQLE*, *FDFT1*, *SCD*, *FADS2*, *LDLR*, *FDPS*, *IDI1*, *HMGCR*, *LSS*, *DHCR24*, *ACAT2* and *FASN*, following TM treatment. In line with this, GSEA revealed that the most enriched biological processes within the genes downregulated by TM were mainly involved in lipid synthesis, such as sterol biosynthetic process, steroid biosynthetic process, activation of gene expression by SREBF and regulation of cholesterol biosynthesis by SREBF. In addition, this finding from whole-genome transcriptome analysis was corroborated by qPCR analysis of individual lipogenic genes over the 4–24 h incubation period. The TM-induced suppression of lipid synthesis contrasts with in vivo studies, which have consistently shown that UPR activation enhances lipogenesis in hepatocytes [43]. In rodent and human liver models, ER stress promotes proteolytic activation of sterol regulatory element-binding protein 1 (SREBF1), a key transcriptional regulator of lipogenic genes such as *ACACA*, *ELOVL6*, *FASN*, and *G6PD* [43–45]. Activation of the ER stress transducer PERK has been shown to be essential for this effect, as PERK deletion reduces expression of lipogenic enzymes including FASN [46].

Interestingly, TG treatment did not affect the expression of genes involved in cholesterol or fatty acid synthesis, despite inducing a similarly strong UPR. This suggests that TM and TG may exert distinct metabolic effects beyond ER stress and UPR activation [26,47]. For instance, TG has been shown to markedly reduce ApoB secretion in Huh7 hepatocytes, whereas TM does not elicit this effect [26]. In order to clarify the divergent effects of TM and TG on lipogenic gene expression, future studies should analyze the activity of SREBF1 by determining the protein levels of precursor (inactive) and nuclear (transcriptionally active) SREBF1. It could be possible that translocation of precursor SREBF1 from the ER to the Golgi apparatus and subsequent site 1 and site 2 protease-mediated processing of SREBF1 is selectively inhibited by TM but not by TG.

Both TM and TG treatments led to upregulation of genes involved in β-oxidation, particularly *CPT1A*, which encodes the rate-limiting enzyme of mitochondrial fatty acid oxidation [48]. This suggests that ER stress promotes β-oxidation in BFH12 cells. Notably, this finding contradicts observations in mice, where hepatic ER stress inhibits mitochondrial β-oxidation [49]. In our study, both TM and TG treatments resulted in reduced intracellular triglyceride levels. For TM, this reduction likely reflects simultaneous inhibition of lipogenesis and stimulation of β-oxidation. For TG, the decrease in triglyceride content may be attributed primarily to enhanced β-oxidation. Future fatty acid oxidation flux experiments using ^{14}C palmitate are warranted to clarify if β-oxidation is enhanced by ER stress inducers.

The implications of these findings for lipid metabolism under ER stress remain unclear. However, a potential link to FGF21, a stress-responsive hormone, may exist. FGF21 is induced by various stress conditions—including environmental, nutritional (fasting, malnutrition, high-fat diet, obesity, amino acid deprivation), and physical exercise—and is also upregulated by ER stress via activating transcription factor 4 (ATF4) [50–52]. FGF21 plays a pivotal role in hepatic energy homeostasis by stimulating β-oxidation, suppressing de novo lipogenesis, and promoting ketogenesis [53,54]. Exogenous FGF21 administration has been shown to reduce hepatic lipid content [55]. There is evidence that FGF21 expression under ER stress may serve as a negative feedback mechanism to mitigate ER stress effects [56].

In our study, ER stress induction by TM and TG led to a dramatic upregulation of *FGF21* expression (5- to 15-fold compared to control), particularly between 4 and 12 h post-treatment. It is conceivable that this robust FGF21 response attenuated the typical ER stress-

induced effects on lipid metabolism, such as increased lipogenesis, suppressed β-oxidation, and elevated intracellular triglyceride levels. In dairy cows, hepatic FGF21 expression also rises sharply during early lactation compared to late gestation—by approximately 10-fold [17] or even 100-fold [18]. If elevated FGF21 expression counteracts ER stress-mediated alterations in lipid metabolism, it may suggest that ER stress does not play a central role in the development of fatty liver in dairy cows.

Studies in rodents have demonstrated that FGF21 also enhances ketogenesis—a metabolic pathway specifically engaged to ensure cerebral energy supply during fasting conditions [57]. Given that ER stress markedly stimulates the release of FGF21, it has been hypothesized that ER stress may promote ketogenesis. However, whole-genome array analysis did not reveal upregulation of genes associated with ketogenesis, including HMG-CoA synthase, the key enzyme in this pathway. Furthermore, qPCR data for *ACAT1* and *HMGCL*, two genes involved in ketogenesis, did not exhibit a consistent pattern of regulation. These findings suggest that ER stress does not induce ketogenesis in BFH12 cells.

Previous studies have shown that ER stress activates the NF-κB signaling pathway via inositol-requiring enzyme 1 alpha, initiating inflammatory responses [58,59]. Our data demonstrate that ER stress induction upregulates *NFKB1* and *TNF* expression, indicating activation of pro-inflammatory signaling. It is well established that dairy cows frequently experience hepatic inflammation during early lactation, which may arise from various sources. Our findings support the notion that ER stress contributes to this pro-inflammatory hepatic condition, alongside other factors such as oxidative stress, social stress, heat stress, leaky gut syndrome, metritis, and mastitis [8].

ER stress is also known to activate Nrf2, a transcription factor that regulates the expression of antioxidant and cytoprotective genes. Under basal conditions, Nrf2 is sequestered by its inhibitor Keap1. Upon ER stress, PERK-mediated phosphorylation of Nrf2 disrupts the Nrf2–Keap1 complex, allowing Nrf2 to translocate to the nucleus and activate transcription of genes containing antioxidant response elements in their promoters [11,60]. Activation of the Nrf2 pathway may serve to counteract ER stress-inducing factors such as oxidative stress and inflammation. Contrary to these reports, our study found that TM and TG treatments led to downregulation of several Nrf2-regulated antioxidant genes (*CAT*, *GPX3*, *NQO1*, *SOD1*). Although we did not directly assess Nrf2 activity, these findings suggest that Nrf2 signaling was not activated in BFH12 cells under ER stress conditions. Our investigation suggests that ER stress may even impair the antioxidant defense system in BFH12 cells.

One limitation of the study is that the doses of ER stress inducers used caused a slight reduction of cell viability of approximately 20%. Thus, we cannot exclude that at least some of the effects observed were the consequence of cell toxicity. Thus, future studies using chemical chaperones (e.g., TUDCA) should clarify if some of the effects observed (e.g., induction of UPR marker genes, reduction of lipogenesis) are reversible. Another limitation of this study is that ER stress in BFH12 cells was induced using synthetic ER stress inducers, which only partially reflects the physiological situation in the liver of freshly lactating dairy cows, where metabolic stressors such as elevated blood levels of NEFA are suspected to act as ER stress inducers. On the other hand, the model used—with TM and TG—offers the advantage of inducing the various ER stress signaling pathways in a much more specific manner, allowing for a more precise investigation of the effects of ER stress on other metabolic pathways compared to the use of NEFA. Unlike TM and TG, NEFA affect numerous additional cellular signaling pathways through activation of several fatty acid–regulated hepatic transcription factors, including peroxisome proliferator-activated receptors α, β, γ1 and γ2, hepatocyte nuclear factor 4 (α and γ), retinoid X-receptor α,

and liver X receptor α and β [61], meaning that the metabolic effects observed during incubation of BFH12 cells with NEFA cannot be attributed solely to ER stress. Moreover, a limitation of the cell model is that the BFH12 cells are of fetal origin and therefore may not fully replicate the metabolic response of mature hepatocytes from freshly lactating dairy cows in all aspects.

5. Conclusions

It was demonstrated that ER stress can be successfully induced in BFH12 cells by incubation with TG or TM. Although BFH12 cells have been proposed as an in vitro model for hepatic steatosis in dairy cows, several hallmark effects of ER stress observed in rodent models—such as the activation of lipogenesis, inhibition of β-oxidation, and induction of the transcription factor Nrf2—could not be replicated in this bovine liver cell line. Extrapolating these findings to the bovine organism suggests that ER stress may not play a central role in the development of fatty liver in dairy cows. However, our data provide indications that ER stress might contribute to the establishment of a pro-oxidant and pro-inflammatory state during early lactation in dairy cattle.

Supplementary Materials: The following supporting information can be downloaded at: https://www.mdpi.com/article/10.3390/dairy6060064/s1, Table S1: Characteristics of gene-specific primers used for qPCR analysis; Table S2: The FC and *p*-value of all differentially expressed transcripts between TM vs. DMSO (Filter settings: $p < 0.05$; FC > 2 or FC < −2); Table S3: The FC and *p*-value of all differentially expressed transcripts between TG vs. DMSO (Filter settings: $p < 0.05$; FC > 2 or FC < −2).

Author Contributions: Conceptualization, D.K.G., R.R. and K.E.; methodology, E.B. and G.W.; software, E.B., R.R. and S.M.G.; validation, D.K.G., R.R. and K.E.; formal analysis, E.B. and G.W.; investigation, E.B., G.W. and D.K.G.; resources, K.E.; data curation, E.B., G.W., S.M.G. and D.K.G.; writing—original draft preparation, E.B., R.R., S.M.G. and K.E.; writing—review and editing, G.W. and D.K.G.; visualization, R.R.; supervision, G.W., D.K.G. and K.E.; project administration, D.K.G. and K.E.; funding acquisition, D.K.G. and K.E. All authors have read and agreed to the published version of the manuscript.

Funding: This research was funded by LOEWE priority program 'GreenDairy—Integrated Livestock-Plant-Agroecosystems' of Hesse's Ministry of Higher Education, Research, and the Arts, grant number LOEWE/2/14/519/03/07.001-(0007)/80.

Institutional Review Board Statement: Not applicable.

Informed Consent Statement: Not applicable.

Data Availability Statement: The microarray data presented in this study are openly available in [NCBI's Gene Expression Omnibus (GEO) repository] at [https://www.ncbi.nlm.nih.gov/geo/query/acc.cgi?acc=GSE305850, accessed on 19 August 2025], reference number [GEO Accession number GSE305850].

Conflicts of Interest: The authors declare no conflicts of interest.

Abbreviations

The following abbreviations are used in this manuscript:

ER	Endoplasmic reticulum
FGF21	Fibroblast growth factor 21
NEB	Negative energy balance
NEFAs	Non-esterified fatty acids
NF-kB	nuclear factor kappa B
Nrf2	nuclear factor erythroid 2-related factor 2

TG	Thapsigargin
TM	Tunicamycin
UPR	Unfolded protein response

References

1. Drackley, J.K. Biology of Dairy Cows during the Transition Period: The Final Frontier? *J. Dairy Sci.* **1999**, *82*, 2259–2273. [CrossRef]
2. Drackley, J.K.; Overton, T.R.; Douglas, G.N. Adaptations of Glucose and Long-Chain Fatty Acid Metabolism in Liver of Dairy Cows during the Periparturient Period. *J. Dairy Sci.* **2001**, *84*, E100–E112. [CrossRef]
3. Gross, J.J. Hepatic Lipidosis in Ruminants. *Vet. Clin. N. Am. Food Anim. Pract.* **2023**, *39*, 371–383. [CrossRef]
4. McArt, J.A.A.; Nydam, D.V.; Oetzel, G.R.; Overton, T.R.; Ospina, P.A. Elevated Nonesterified Fatty Acids and β-Hydroxybutyrate and Their Association with Transition Dairy Cow Performance. *Vet. J.* **2013**, *198*, 560–570. [CrossRef]
5. Plaizier, J.C.; Krause, D.O.; Gozho, G.N.; McBride, B.W. Subacute Ruminal Acidosis in Dairy Cows: Physiological Causes, Incidence and Consequences. *Vet. J.* **2008**, *176*, 21–31. [CrossRef]
6. Vels, L.; Røntved, C.M.; Bjerring, M.; Ingvartsen, K.L. Cytokine and Acute Phase Protein Gene Expression in Repeated Liver Biopsies of Dairy Cows with a Lipopolysaccharide-Induced Mastitis. *J. Dairy Sci.* **2009**, *92*, 922–934. [CrossRef]
7. Zebeli, Q.; Metzler-Zebeli, B.U. Interplay between Rumen Digestive Disorders and Diet-Induced Inflammation in Dairy Cattle. *Res. Vet. Sci.* **2012**, *93*, 1099–1108. [CrossRef]
8. Bradford, B.J.; Yuan, K.; Farney, J.K.; Mamedova, L.K.; Carpenter, A.J. Invited review: Inflammation during the Transition to Lactation: New Adventures with an Old Flame. *J. Dairy Sci.* **2015**, *98*, 6631–6650. [CrossRef]
9. Gessner, D.K.; Schlegel, G.; Ringseis, R.; Schwarz, F.J.; Eder, K. Up-Regulation of Endoplasmic Reticulum Stress-Induced Genes of the Unfolded Protein Response in the Liver of Periparturient Dairy Cows. *BMC Vet. Res.* **2014**, *10*, 46. [CrossRef]
10. Yonekura, S. The Role of Endoplasmic Reticulum Stress in Metabolic Diseases and Mammary Epithelial Cell Homeostasis in Dairy Cows. *Anim. Sci. J.* **2024**, *95*, e13935. [CrossRef]
11. Cnop, M.; Foufelle, F.; Velloso, L.A. Endoplasmic Reticulum Stress, Obesity and Diabetes. *Trends Mol. Med.* **2012**, *18*, 59–68. [CrossRef] [PubMed]
12. Marciniak, S.J.; Ron, D. Endoplasmic reticulum stress signaling in disease. *Physiol. Rev.* **2006**, *86*, 1133–1149. [CrossRef]
13. Ron, D.; Walter, P. Signal integration in the endoplasmic reticulum unfolded protein response. *Nat. Rev. Mol. Cell Biol.* **2007**, *8*, 519–529. [CrossRef]
14. Cullinan, S.B.; Diehl, J.A. Coordination of ER and oxidative stress signaling: The PERK/Nrf2 signaling pathway. *Int. J. Biochem. Cell Biol.* **2006**, *38*, 317–332. [CrossRef]
15. Zhang, K.; Kaufman, R.J. From endoplasmic-reticulum stress to the inflammatory response. *Nature* **2008**, *454*, 455–462. [CrossRef]
16. Erickson, A.; Moreau, R. The regulation of FGF21 gene expression by metabolic factors and nutrients. *Horm. Mol. Biol. Clin. Investig.* **2016**, *30*, 20160016. [CrossRef]
17. Schoenberg, K.M.; Giesy, S.L.; Harvatine, K.J.; Waldron, M.R.; Cheng, C.; Kharitonenkov, A.; Boisclair, Y.R. Plasma FGF21 Is Elevated by the Intense Lipid Mobilization of Lactation. *Endocrinology* **2011**, *152*, 4652–4661. [CrossRef]
18. Schlegel, G.; Ringseis, R.; Keller, J.; Schwarz, F.J.; Windisch, W.; Eder, K. Expression of Fibroblast Growth Factor 21 in Liver of Dairy Cows during Transition and Lactation. *J. Anim. Physiol. Anim. Nutr.* **2013**, *97*, 820–829. [CrossRef]
19. Kim, K.H.; Lee, M.S. FGF21 as a Mediator of Adaptive Responses to Stress and Metabolic Benefits of Anti-Diabetic Drugs. *J. Endocrinol.* **2015**, *226*, R1–R16. [CrossRef] [PubMed]
20. Eder, K.; Gessner, D.K.; Ringseis, R. Fibroblast Growth Factor 21 in Dairy Cows: Current Knowledge and Potential Relevance. *J. Anim. Sci. Biotechnol.* **2021**, *12*, 97. [CrossRef] [PubMed]
21. Gessner, D.K.; Sandrock, L.M.; Most, E.; Koch, C.; Ringseis, R.; Eder, K. Performance and metabolic, inflammatory, and oxidative stress-related parameters in early lactating dairy cows with high and low hepatic FGF21 expression. *Animals* **2022**, *13*, 131. [CrossRef] [PubMed]
22. Ringseis, R.; Gessner, D.K.; Eder, K. Molecular Insights into Liver-Associated Diseases in Early-Lactating Dairy Cows: Hypothetical Role of Endoplasmic Reticulum Stress. *J. Anim. Physiol. Anim. Nutr.* **2015**, *99*, 626–645. [CrossRef]
23. Yoshida, H. ER Stress and Diseases. *FEBS J.* **2007**, *274*, 630–658. [CrossRef]
24. Reichelt, K.; Niebisch, A.M.; Kacza, J.; Schoeniger, A.; Fuhrmann, H. The Bovine Hepatic Cell Line BFH12 as a Possible Model for Hepatosteatosis in Dairy Cows. *Front. Vet. Sci.* **2022**, *9*, 840202. [CrossRef]
25. Foufelle, F.; Fromenty, B. Role of Endoplasmic Reticulum Stress in Drug-Induced Toxicity. *Pharmacol. Res. Perspect.* **2016**, *4*, e00211. [CrossRef]
26. Otaibi, A.A.; Mubarak, S.A.S.; Hejji, F.A.; Almasaud, A.; Jami, H.A.; Iqbal, J.; Quarni, A.A.; Harbi, N.K.A.; Bakillah, A. Thapsigargin and Tunicamycin block SARS-CoV-2 entry into host cells via differential modulation of unfolded protein response (UPR), AKT signalling, and apoptosis. *Cells* **2024**, *13*, 769. [CrossRef]

27. Gleich, A.; Kaiser, B.; Schumann, J.; Fuhrmann, H. Establishment and characterisation of a novel bovine SV40 large T-antigen-transduced foetal hepatocyte-derived cell line. *Vitr. Cell. Dev. Biol. Anim.* **2016**, *52*, 662–672. [CrossRef]
28. Chiappisi, E.; Ringseis, R.; Eder, K.; Gessner, D.K. Effect of ER Stress on Metabolic Signaling and Kidney-Specific Functions in MDBK Cells. *J. Dairy. Sci.* **2017**, *100*, 6689–6706. [CrossRef] [PubMed]
29. Beller, S.; Grundmann, S.M.; Pies, K.; Most, E.; Schuchardt, S.; Seel, W.; Simon, M.C.; Eder, K.; Ringseis, R. Effect of replacing soybean meal with Hermetia illucens meal on cecal microbiota, liver transcriptome, and plasma metabolome of broilers. *Poult. Sci.* **2024**, *103*, 103635. [CrossRef]
30. Edgar, R.; Domrachev, M.; Lash, A.E. Gene expression Omnibus: NCBI gene expression and hybridization array data repository. *Nucleic Acids Res.* **2002**, *30*, 207–210. [CrossRef] [PubMed]
31. Xu, S.; Hu, E.; Cai, Y.; Xie, Z.; Luo, X.; Zhan, L.; Tang, W.; Wang, Q.; Liu, B.; Wang, R.; et al. Using clusterProfiler to characterize multiomics data. *Nat. Protoc.* **2024**, *19*, 3292–3320. [CrossRef]
32. Subramanian, A.; Tamayo, P.; Mootha, V.K.; Mukherjee, S.; Ebert, B.L.; Gillette, M.A.; Paulovich, A.; Pomeroy, S.L.; Golub, T.R.; Lander, E.S.; et al. Gene set enrichment analysis: A knowledge-based approach for interpreting genome-wide expression profiles. *Proc. Natl. Acad. Sci. USA* **2005**, *102*, 15545–15550. [CrossRef]
33. Liberzon, A.; Birger, C.; Thorvaldsdóttir, H.; Ghandi, M.; Mesirov, J.P.; Tamayo, P. The Molecular Signatures Database hallmark gene set collection. *Cell Syst.* **2015**, *1*, 417–425. [CrossRef]
34. Liberzon, A.; Subramanian, A.; Pinchback, R.; Thorvaldsdóttir, H.; Tamayo, P.; Mesirov, J.P. Molecular signatures database (MSigDB) 3.0. *Bioinformatics* **2011**, *27*, 1739–1740. [CrossRef] [PubMed]
35. Dolgalev, I. Msigdbr: MSigDB Gene Sets for Multiple Organisms in a Tidy Data Format. R Package Version 25.1.1. 2025. Available online: https://igordot.github.io/msigdbr/ (accessed on 18 October 2025).
36. R Core Team. *R: A Language and Environment for Statistical Computing*; R Foundation for Statistical Computing: Vienna, Austria, 2025. Available online: https://www.R-project.org/ (accessed on 18 October 2025).
37. Rozen, S.; Skaletsky, H. *Primer3 on the WWW for General Users and for Biologist Programmers*; Krawetz, S., Misener, S., Eds.; Bioinformatics Methods and Protocols: Methods in Molecular Biology; Humana Press: Totowa, NJ, USA, 2000; pp. 365–386.
38. Altschul, S.F.; Gish, W.; Miller, W.; Myers, E.W.; Lipman, D.J. Basic local alignment search tool. *J. Mol. Biol.* **1990**, *215*, 403–410. [CrossRef] [PubMed]
39. Vandesompele, J.; de Preter, K.; Pattyn, F.; Poppe, B.; van Roy, N.; de Paepe, A.; Speleman, F. Accurate normalization of real-time quantitative RT-PCR data by geometric averaging of multiple internal control genes. *Genome Biol.* **2002**, *3*, RESEARCH0034. [CrossRef]
40. Wen, G.; Eder, K.; Ringseis, R. Resveratrol Alleviates ER Stress-Induced Inhibition of Thyroid Hormone Synthesis Genes in FRTL-5 Thyrocytes. *Int. J. Mol. Sci.* **2021**, *22*, 4373. [CrossRef]
41. Wen, G.; Eder, K.; Ringseis, R. Comparative evaluation of the modulatory role of 1,25-dihydroxy-vitamin D3 on endoplasmic reticulum stress-induced effects in 2D and 3D cultures of the intestinal porcine epithelial cell line IPEC-J2. *J. Anim. Sci. Biotechnol.* **2024**, *15*, 153. [CrossRef] [PubMed]
42. Busato, S.; Bionaz, M. The Interplay between Non-Esterified Fatty Acids and Bovine PPARs: Results of an In Vitro Hybrid Approach. *J. Anim. Sci. Biotechnol.* **2020**, *11*, 91. [CrossRef]
43. Ferré, P.; Foufelle, F. Hepatic Steatosis: Role of De Novo Lipogenesis and SREBP-1c. *Diabetes Obes. Metab.* **2010**, *12* (Suppl. S2), 83–92. [CrossRef]
44. Fang, D.L.; Wan, Y.; Shen, W.; Cao, J.; Sun, Z.-X.; Yu, H.-H.; Zhang, Q.; Cheng, W.-H.; Cheng, W.-H.; Chen, J.; et al. ER Stress Leads to Lipid Accumulation via SREBP-1c Upregulation. *Mol. Cell. Biochem.* **2013**, *381*, 127–137. [CrossRef]
45. Kammoun, H.L.; Hainault, I.; Ferré, P.; Foufelle, F. Nutritional Liver Disease: Targeting ER Stress. *Curr. Opin. Clin. Nutr. Metab. Care* **2009**, *12*, 575–582.
46. Bobrovnikova-Marjon, E.; Hatzivassiliou, G.; Grigoriadou, C.; Romero, M.; Cavener, D.R.; Thompson, C.B.; Diehl, J.A. PERK-dependent regulation of lipogenesis during mouse mammary gland development and adipocyte differentiation. *Proc. Natl. Acad. Sci. USA* **2008**, *105*, 16314–16319. [CrossRef]
47. Mendez, J.M.; Kolora, L.D.; Lemon, J.S.; Dupree, S.L.; Keestra-Gounder, A.M. ER Stress Response Impacts NOD1 Signaling. *Infect. Immun.* **2019**, *87*, e00826-18. [CrossRef] [PubMed]
48. Schlaepfer, I.R.; Joshi, M. CPT1A-Mediated Fat Oxidation: Mechanisms and Therapeutic Potential. *Endocrinology* **2020**, *161*, bqz046. [CrossRef] [PubMed]
49. DeZwaan-McCabe, D.; Sheldon, R.D.; Gorecki, M.C.; Guo, D.F.; Gansemer, E.R.; Kaufman, R.J.; Rahmouni, K.; Gillum, M.P.; Taylor, E.B.; Teesch, L.M.; et al. ER Stress Inhibits Liver Fatty Acid Oxidation and Induces Steatosis. *Cell Rep.* **2017**, *19*, 1794–1806. [CrossRef] [PubMed]
50. Schaap, F.G.; Kremer, A.E.; Lamers, W.H.; Jansen, P.L.M.; Gaemers, I.C. FGF21 Is Induced by ER Stress. *Biochimie* **2013**, *95*, 692–699. [CrossRef]

51. Jiang, S.; Yan, C.; Fang, Q.C.; Shao, M.L.; Zhang, Y.L.; Liu, Y.; Deng, Y.P.; Shan, B.; Liu, J.Q.; Li, H.T.; et al. FGF21 Regulated by IRE1α-XBP1 Counteracts ER Stress-Induced Hepatic Steatosis. *J. Biol. Chem.* **2014**, *289*, 29751–29765. [CrossRef]
52. Wan, X.S.; Lu, X.H.; Xiao, Y.C.; Lin, Y.; Zhu, H.; Ding, T.; Yang, Y.; Huang, Y.; Zhang, Y.; Liu, Y.L.; et al. ATF4- and CHOP-dependent induction of FGF21 via ER stress. *Biomed. Res. Int.* **2014**, *2014*, 807874. [CrossRef]
53. Owen, B.M.; Mangelsdorf, D.J.; Kliewer, S.A. Tissue-specific actions of FGF15/19 and FGF21. *Trends Endocrinol. Metab.* **2015**, *26*, 22–29. [CrossRef]
54. Barros, D.R.; Hegele, R.A. FGF21: Update on genetics and molecular biology. *Curr. Opin. Lipidol.* **2025**, *36*, 88–95. [CrossRef]
55. Tillman, E.J.; Rolph, T. FGF21: Emerging Therapeutic Target for NASH and Metabolic Diseases. *Front. Endocrinol.* **2020**, *11*, 601290. [CrossRef]
56. Maruyama, R.; Shimizu, M.; Hashidume, T.; Inoue, J.; Itoh, N.; Sato, R. FGF21 alleviates hepatic ER stress under physiological conditions. *J. Nutr. Sci. Vitaminol.* **2018**, *64*, 200–208. [CrossRef] [PubMed]
57. Iglesias, P.; Selgas, R.; Romero, S.; Diez, J.J. Mechanisms in Endocrinology: Biological role, clinical significance, and therapeutic possibilities of the recently discovered metabolic hormone fibroblastic growth factor 21. *Eur. J. Endocrinol.* **2012**, *167*, 301–309. [CrossRef] [PubMed]
58. Malhi, H.; Kaufman, R.J. Endoplasmic reticulum stress in liver disease. *J. Hepatol.* **2011**, *54*, 795–809. [CrossRef] [PubMed]
59. Zheng, T.; Huang, K.Y.; Tang, X.D.; Wang, F.Y.; Lv, L. Endoplasmic reticulum stress in gut inflammation: Implications for ulcerative colitis and Crohn's disease. *World J. Gastroenterol.* **2025**, *31*, 10467–10471. [CrossRef]
60. Cullinan, S.B.; Zhang, D.; Hannink, M.; Arvisais, E.; Kaufman, R.J.; Diehl, J.A. Nrf2 Is a Direct PERK Substrate and Effector of Cell Survival. *Mol. Cell. Biol.* **2003**, *23*, 7198–7208. [CrossRef]
61. Jump, D.B.; Tripathy, S.; Depner, C.M. Fatty acid-regulated transcription factors in the liver. *Annu. Rev. Nutr.* **2013**, *33*, 249–269. [CrossRef]

Disclaimer/Publisher's Note: The statements, opinions and data contained in all publications are solely those of the individual author(s) and contributor(s) and not of MDPI and/or the editor(s). MDPI and/or the editor(s) disclaim responsibility for any injury to people or property resulting from any ideas, methods, instructions or products referred to in the content.